Trakya University Journal of Natural Sciences, 27(1), 104–114, 2026
DOI: 10.23902/trkjnat.2025121
www.tujns.org

Research Article

Interaction between circadian gene *Bmal1* and adipogenic regulator *PPARγ* in UVB-exposed mesenchymal stem cells

Afra Keban, Elçin Tank, Beril Erdem, Esin Akbay Çetin*

Hacettepe University, Faculty of Science, Department of Biology, Ankara, Türkiye

Cite this article as: Keban, A., Tank, E., Erdem, B., & Akbay Çetin, E. (2026). Interaction between circadian gene *Bmal1* and adipogenic regulator *PPARγ* in UVB-exposed mesenchymal stem cells. *Trakya University Journal of Natural Sciences, 27*(1), 104–114. https://doi.org/10.23902/trkjnat.2025121

Abstract

Background: Mesenchymal stem cells (MSCs), including adipose-derived MSCs (ADMSCs) and bone marrow-derived MSCs (BMMSCs), are multipotent cells essential for tissue repair, with strong self-renewal and differentiation abilities. *Bmal1* is a core component of the circadian cycle and plays a regulatory role in stem cell specialization; *PPARγ* links adipogenesis to the circadian rhythm by epigenetically regulating *Bmal1*. Ultraviolet B (UVB) radiation influences circadian processes by modulating the expression of growth factors and cytokines in MSCs.

Aims: This study investigated how UVB affects adipogenesis and circadian-system-related gene transcription in ADMSCs and BMMSCs.

Methods: MSC viability post-exposure was assessed using 3-(4,5-dimethylthiazol-2-yl)-2,5-diphenyltetrazolium bromide analysis. Cells were cultured in adipogenesis medium and stained with Oil Red O at multiple time points. UVB-treated MSCs were maintained under differentiation-inducing conditions for 28 days, and gene expression was evaluated by quantitative real-time polymerase chain reaction (qRT-PCR).

Results: Viability assays identified 25 mJ/cm² as the optimal UVB dose. Flow cytometry confirmed the enhanced expression of MSC markers (CD54, CD90, and CD29) and low expression of hematopoietic markers (CD45, CD106, and MHC class II). Oil Red O staining revealed gradual lipid accumulation, beginning on day 14 and forming mature droplets by day 28. qRT-PCR indicated a significant increase in *PPARγ* expression in adipogenic differentiation groups and *Bmal1* expression post-UVB exposure.

Özet

Dayanak: Yağ dokusundan elde edilen mezenkimal kök hücreler (ADMKH) ve kemik iliğinden elde edilen mezenkimal kök hücreler (KİMKH) dâhil olmak üzere mezenkimal kök hücreler (MKH), güçlü öz yenilenme ve farklılaşma kapasiteleri sayesinde doku onarımında önemli rol oynayan multipotent hücrelerdir. *Bmal1* proteini, günlük hücresel biyolojik süreçleri düzenleyen sirkadiyen döngünün temel bileşenlerinden biridir ve baskılanmasının kök hücrelerin farklılaşma kapasitesini değiştirdiği bilinmektedir. *PPARγ* ise adipojenik farklılaşma ile sirkadiyen ritim arasında bağlantı kurarak *Bmal1*'in epigenetik düzenlenmesinde rol oynamaktadır. Ultraviyole B (UVB) radyasyonunun, MKH'lerde büyüme faktörleri ve sitokin ekspresyonunu etkileyerek sirkadiyen ritim üzerinde etkili olduğu bilinmektedir.

Amaçlar: Bu çalışmada, ADMKH ve KİMKH'lerde UVB ışığının hücre farklılaşması ve sirkadiyen ritim üzerindeki etkileri araştırılmıştır.

Yöntemler: UV ışığına maruz bırakılan MKH'lerin canlılık potansiyelleri MTT analizi ile değerlendirilmiştir. Hücreler adipojenik farklılaşma ortamında kültürlenmiş ve farklı günlerde Oil Red O boyaması yapılmıştır. UVB'ye maruz kalan MKH'ler, farklılaşma ortamında 28 gün boyunca takip edilmiş ve gen ekspresyonundaki değişiklikler kantitatif gerçek zamanlı polimeraz zincir reaksiyonu (qRT-PCR) yöntemiyle analiz edilmiştir.

Bulgular: Sonuç olarak, hücre canlılığı analizleri optimal UVB dozunun 25 mJ/cm² olduğunu göstermiştir. Akış sitometrisi sonuçları, MKH fenotipine özgü belirteçlerin (CD54, CD90, CD29) yüksek düzeyde, hematopoietik belirteçlerin (CD45, CD106, MHC sınıf II) ise düşük düzeyde eksprese edildiğini ortaya koymuştur. Oil Red O

Edited by: *Reşat Ünal*

***Corresponding Author:** Esin Akbay Çetin, **E-mail:** akbayesin@gmail.com*

***ORCID iDs of the author(s):** AK. 0009-0000-1379-0759; ET. 0009-0006-1346-4965; BE. 0000-0002-9820-1147; EAÇ. 0000-0002-0797-8322*

Received: 2 December 2025, **Accepted:** 20 March 2026, **Epub:** 13 April 2026, **Published:** 24 April 2026

Conclusion: Overall, these findings suggest that UVB stimulation at optimal doses enhances the adipogenic differentiation capacity of MSCs while modulating circadian rhythm-associated genes. Moreover, adipogenic differentiation itself appears to contribute to the regulation of the circadian rhythm.

boyaması ile 14. günden itibaren lipit birikimi gözlenmiş, 28. günde ise olgun yağ damlacıkları tespit edilmiştir. qRT-PCR sonuçlarına göre, adipojenik farklılaşma gruplarında *PPARγ* ekspresyonu anlamlı düzeyde artarken, *Bmal1* ekspresyonunun da UVB uygulaması sonrasında arttığı belirlenmiştir.

Sonuç: Elde edilen bulgular, optimal UVB dozunun MKH'lerin adipojenik farklılaşmasını desteklediğini ve sirkadiyen ritmi düzenlediğini göstermektedir. Ayrıca, bu çalışma adipojenik farklılaşmanın sirkadiyen ritim üzerinde düzenleyici bir etkisi olduğunu da ortaya koymaktadır.

Keywords: Mesenchymal stem cell, *Bmal1*, *PPARγ*, ultraviolet light, qRT-PCR

Introduction

Mesenchymal stem cells (MSCs) are multipotent progenitor cells capable of self-renewal and differentiation into multiple mesodermal lineages, including adipocytes, osteoblasts, and chondrocytes (Česnik and Švajger, 2024). In addition, MSCs secrete a wide variety of growth factors and cytokines that contribute to tissue repair and regeneration, making them a commonly used experimental model in regenerative medicine and developmental biology (Pittenger et al., 2019; Vilar et al., 2023). The differentiation fate of MSCs is tightly regulated by mechanisms such as signaling pathways, cell-cycle regulators, microRNAs, transcription factors, and epigenetic modifications (Mens and Ghanbari, 2018). MSCs can be isolated from several tissues, most commonly bone marrow and adipose tissue. Bone marrow-derived MSCs (BMMSCs) exhibit low immunogenicity, multilineage differentiation potential, and robust migratory capacity. Adipose-derived MSCs (ADMSCs) are abundant, easily accessible, and relatively unaffected by donor age. Although MSCs from different tissues share core stem cell characteristics, subtle variations in marker expression and differentiation tendencies render tissue origin a crucial factor in stem cell biology studies (Lotfy et al., 2019; Sachs et al., 2025). For these reasons, MSCs represent an appropriate and physiologically relevant model for investigating molecular mechanisms regulating differentiation and cell-level responses to environmental stimuli.

Circadian rhythm and cell-cycle regulation constitute two fundamental interconnected regulatory systems in eukaryotes, operating from an organismal to the molecular level. Circadian rhythms follow a near-24-hour oscillation pattern of alternating active and inactive phases governed by a core molecular clock comprising transcription–translation feedback loops (Putthanbut et al., 2025; Zeng et al., 2024). Key clock genes include *Bmal1*, *Clock*, *Period* (*Per*), *Cryptochrome* (*Cry*), *RORα/β/γ*, and *Rev-erbα/β* (Göncü & Öztürk, 2019). Of these, Brain and Muscle ARNT-Like 1 (*Bmal1*) functions as a central indispensable regulator of the circadian clock. *Bmal1* heterodimerizes with *Clock*, driving rhythmic transcription of downstream clock-controlled genes. Crucially, evidence indicates that *Bmal1* is essential for maintaining diurnal rhythmicity and plays a critical role in fate determination and differentiation of stem cells. Suppressed or disrupted *Bmal1* expression in stem cells impairs lineage-specific gene activation, alters the metabolic program, and compromises differentiation efficiency (Gao et al., 2022). Therefore, in this study, *Bmal1* was selected as a key molecular link between circadian regulation, cell metabolism, and differentiation.

Adipogenesis was specifically investigated as it is one of the most well-characterized and metabolically sensitive MSC-differentiation pathways. This process is tightly controlled by both circadian clock-associated genes and metabolism-related transcription factors, making it an ideal model for exploring clock–metabolism interactions. Peroxisome proliferator-activated receptor gamma (*PPARγ*) is the master regulator of adipocyte differentiation and governs lipid storage, insulin sensitivity, and glucose metabolism. *PPARγ* activity is influenced by environmental and circadian cues and is modulated through post-translational and epigenetic mechanisms (Montaigne et al., 2021).

Crucially, *PPARγ* represses *Bmal1* transcription in adipocytes, altering cell metabolism, reducing histone acetylation and methylation, and disrupting circadian rhythmicity. *PPARγ* integrates adipogenesis with diurnal clock regulation via this mechanism, establishing a feedback loop between metabolic state, epigenetic modifications, and circadian disruption (Wang et al., 2022). Consequently, adipogenic differentiation provides a biologically relevant context to examine the *Bmal1–PPARγ* interaction under external stimuli. Collectively, these findings suggest the occurrence of such a tightly regulated and bidirectional interconnectivity during adipogenic differentiation (Wang et al., 2022). While *Bmal1* influences metabolic timing and differentiation competence in MSCs (Gao et al., 2022), *PPARγ* is not only a downstream effector of adipogenesis but also an upstream modulator of circadian gene expression through the transcriptional and epigenetic repression of *Bmal1* (Wang et al., 2022). Such a reciprocal regulatory axis positions the *Bmal1–PPARγ* network as a central integrator of circadian rhythm, metabolic state, and cell-differentiation fate (Li et al., 2023a; Montaigne et al., 2021; Takahashi, 2017).

However, the mechanisms by which external stimuli, such as ultraviolet (UV) light modulate this regulatory interplay remain insufficiently understood (Ezati et al., 2023; Liao et al., 2023). UV is a major environmental factor influencing circadian rhythms. Exposure to UV and visible light has been implicated in modulating cell-level metabolism, clock gene expression, and regenerative responses. UVA, ultraviolet B (UVB), and UVC

differ in wavelength: 315–400, 280–315, and 100–280 nm, and bioimpacts (Ezati et al., 2023; Goodenow et al., 2022; Li et al., 2023b; Sani et al., 2024). Controlled UV exposure enhances secretory activity and regenerative potential in MSCs, suggesting a link between UV-induced stress responses and circadian regulation (Liao et al., 2023; Ra et al., 2023).

Therefore, this study aims to investigate how adipogenic differentiation modulates circadian rhythm regulation through a reciprocal interaction between *Bmal1* and *PPARγ* in UV-treated MSCs derived from various tissue sources.

Materials and Methods

Materials

Phosphate-buffered saline (PBS), 0.25% Trypsin-EDTA, 3-(4,5-dimethylthiazol-2-yl) 2,5-diphenyltetrazolium bromide (MTT), 3-isobutyl-1-methylxanthine (IBMX), insulin, and penicillin/streptomycin (P/S) were purchased from Sigma-Aldrich (Merck KGaA, Darmstadt, Germany). Fetal bovine serum (FBS) and Dulbecco's modified Eagle medium/Nutrient Mixture F12 (DMEM/F12) were purchased from Biowest (St. Louis, MO, France). Oil-red O staining solution, RevertAid First Strand cDNA Synthesis Kit, Power SYBR™ Green Master Mix, and culture dishes were obtained from Thermo Fisher Scientific (Waltham, MA, USA). Dexamethasone and indomethacin were purchased from Merck Millipore (St. Louis, MO, France). Xylazine (Rompun®) was bought from Abdi İbrahim İlaç Pazarlama A.Ş. (İstanbul, Türkiye). Ketamine (Ketalar® 50 mg/mL) was obtained from Eczacıbaşı İlaç Pazarlama A.Ş. (Lüleburgaz, Türkiye). All antibodies were purchased from Santa Cruz Biotechnology (Dallas, TX, USA).

MSCs Isolation

MSCs were isolated from three randomly selected 24-week-old male *Wistar albino* rats raised as a single colony. The laboratory was pre-sterilized with UV light for 1 h, and all surgical materials were autoclaved. The animals used were obtained post-approval from the Hacettepe University Animal Ethics Committee (number 2021/05-05; dated June 22, 2021). The rats were anesthetized with xylazine (10 mg/kg) and ketamine (50 mg/kg); lateral and gonadal adipose tissue, femoral, and tibial bones were removed under sterile conditions in a laminar flow cabinet. Adipose tissues were placed in a transport medium containing antibiotics–antimycotics—DMEM/F12 containing 20% FBS and 2% P/S—in a laminar flow cabinet. Tissues were dissected into 4–5 mm-sized pieces and placed in 12-well culture dishes. Then a drop of primary medium was added and incubated for 15 min. Then, after adding enough primary medium to cover the tissue pieces without floating, the incubation was continued (Çetin et al., 2023; Niyaz et al., 2012).

The metaphyzes of the femur and tibia were cut out. The bone marrow was collected using an injector needle, washed with transport medium, and dissected with a scalpel. The tissues were transferred to a medium-containing Falcon tube and centrifuged at 800 rpm for 5 min. The supernatant was removed, and a 1/9 solution of PBS/RBC was added. The tube was kept on ice for 10 min and recentrifuged. The supernatant was collected, suspended three times with 5 mL of medium, and washed by centrifugation. The pellet was suspended with medium in a 6-well culture dish and seeded with 2 mL of medium per well (Sevim et al., 2018).

An equal amount of medium was renewed every day for one week to neutralize the MSC differentiation effect of cytokines. After incubation for a week, changes in cell morphology were examined under an IX70 inverted microscope (Olympus Corporation, Tokyo, Japan). Passaging was performed after the MSCs covered the entire culture dish surface. Based on primary culture and early *in vitro* expansion, $1–5 \times 10^6$ ADMSCs and $0.5–2 \times 10^6$ BMMSCs were obtained between passages 2 and 4, consistent with previous reports (Niyaz et al., 2012), which were used for the experiments.

Characterization and Differentiation Potential of MSCs

MSCs were characterized using flow cytometry. After trypsinization, the MSCs were centrifuged, and fluorescein isothiocyanate-conjugated antibodies were added to the pelleted cells suspended in a wash buffer. The MSCs were then incubated at room temperature for 45 min. For this purpose, antibodies specific to positive and negative markers CD29, CD90, CD54, CD45, CD106, and MHC class II antigens, and isotype controls were used to immunophenotype MSCs.A CytoFLEX LX flow cytometer (Beckman Coulter, IN, USA), and approximately 3×10^5 cells per sample were analyzed. To ensure accurate data interpretation, negative controls, including unstained cells, were employed to define the boundaries of positive signals during the gating process.

For assessing their adipogenic potential, MSCs were seeded at 2×10^4 cells/well in 96-well culture dishes using DMEM/F12 medium supplemented with 10% FBS and 1% (P/S). The cells reached ~80% confluency within 1 day, after which the adipogenic differentiation medium was added. Adipogenesis was induced in the cells of all experimental groups at the same seeding density and at comparable confluency levels; they were cultured for 28 days. Adipogenic medium was prepared by adding 10^{-7} M dexamethasone, 5 µg/mL insulin, 60 µM indomethacin, and 500 µM IBMX to DMEM medium. The medium was changed every two days, and differentiation was examined by Oil Red O staining. Briefly, the medium was removed, and the dish was washed with PBS. Then, 100 µL 10% formalin was added, incubated for 5 min, and washed with distilled water, followed with 60% isopropanol. Oil Red O was added to cover the surface and left aside for 15 min. It was then washed with 60% isopropanol alcohol until the color lightened. Hematoxylin was added to cover the surface and left aside for 10 s. It was washed now with distilled water until the color diminished. The stained wells were covered with PBS and visualized with an Olympus IX70 inverted microscope at X20 magnification. The software ImageJ, version 1.54p (NIH, USA), was used to quantitatively analyze the intensity and distribution of red color in selected images. In brief, three areas from representative sections of each sample were randomly selected. Then, the surface area of

the stained portion was compared to the total matrix area and expressed as a ratio (Zhu et al., 2022).

UV Application and Cell Viability Assay

The ADMSCs and BMMSCs were seeded for 24 h in 96-well culture dishes, the medium was then collected, and then the cells were covered with sterile PBS. UVB at doses of 25, 50, and 100 mJ/cm² were applied for 17, 34, and 68 s, respectively. UV was provided with a Philips PL-S 9W\01 ampoule. PBS was replaced, MTT was added, and incubated at 0, 24, and 48 h to analyze cell viability. The optimum UVB dose was defined as the highest one that preserved cell viability without inducing significant cytotoxicity and was used in all experiments.

For the MTT assay, the culture medium was replaced with a medium-containing MTT/DMEM (serum-free) solution at 1:10 and incubated for 2–4 h under standard conditions. The formazan crystals formed were dissolved by replacing the medium with isopropyl alcohol. OD_{570} nm was measured with an EZ Read 400 ELISA microplate reader (Biochrom Ltd., Cambridge, UK). The viability of the treated groups was calculated as a percentage of the control group.

Quantitative Real-Time Polymerase Chain Reaction (qRT-PCR) Analysis

ADMSCs and BMMSCs were seeded into culture dishes for 24 h. After UVB treatment, adipogenic differentiation medium was added to culture dishes, and the medium was renewed every two days for 28 days. At the end of this period, the expression of *Bmal1* and *PPARγ* genes was quantified by qRT-PCR. First, RNA was isolated from the MSCs using Trizol and converted into cDNA using the RevertAid First Strand cDNA synthesis kit (Thermo Fisher Scientific) and a BIO-RAD T100 Thermal Cycler. *Bmal1* and *PPARγ* expression was quantified using Power SYBR Green PCR Master Mix (Thermo Fisher Scientific) with the 7500 Fast & 7500 RT-PCR Systems (Thermo Fisher Scientific), *β-actin* served as a reference gene. ΔΔCt values were calculated, and data were statistically analyzed. The sequences of all primers used are given in Table 1.

Table 1. Sequences of gene-specific primers.

Primer name	Sequence (5'–3')
Bmal1 forward	TGCCACTGACTACCAAGAAAGT
Bmal1 reverse	AACTTCCGGGACATCGCATT
PPARγ forward	CTGCGTCCCCGCCTTAT
PPARγ reverse	TTCAATCGGATGGTTCTTCG
β-actin forward	GGGTTACGCGCTCCCTCATG
β-actin reverse	CCACGCTCGGTCAGGATCTTC

Statistical Analysis

Statistical analysis was performed using GraphPad Prism 8.02 (GraphPad Software Inc., San Diego, CA, USA). Inter-group differences were analyzed by one-way analysis of variance followed by Dunnett's post hoc test for multiple comparisons. Data are presented as the mean ± standard deviation, and a p-value of <0.05 was considered statistically significant.

Results

MSCs Isolation Results

Rat flank and gonadal adipose, and the femur and tibia marrow tissues were extracted under sterile conditions, and incubated in culture dishes under an appropriate environment. The confluent state of the cells was observed under a microscope on pre-selected days. MSCs had started to adhere to the culture dish within 24 h of addition. On the 6th day, they took the shape and form of colonies (Figure 1a and 1b).

Characterization and Differentiation Potential of MSCs

Flow cytometry was used to characterize the MSCs in the P2–P4 stages. The phenotype positive antigens (≥95%): CD54, CD90, and CD29; and phenotype negative antigens (≤7%): CD45, CD106, and MHC class II on the MSC surface were analyzed (Figure 2).

The potential of ADMSCs and BMMSCs to differentiate into adipogenic cells was demonstrated based on the accumulation of lipid vacuoles via Oil Red O staining performed on days 14, 21, and 28. From the 14th day onward, lipid droplets started to appear. Adipogenesis was most intense on the 28th day, at which the cytoplasm was filled with lipid droplets, and the nucleus was rendered peripheral (Figure 1c and 1d). The lipid contents determined support the qualitative observations. Compared to their respective controls, on days 14, 21, and 28, adipogenesis in ADMSCs and BMMSCs occurred at statistically significant levels in each treatment group ($p \leq 0.0001$) (Figure 3).

UV Application and Cell Viability Assay

An optimization protocol was employed to determine the appropriate UVB dose in MSCs. Cells were treated with 25, 50, and 100 mJ/cm^2 doses for 17, 34, and 68 s, and viability was measured by assaying mitochondrial activity (Figure 4). MTT assay was performed at 0, 24, and 48 h. Cell viability was the highest at 25 mJ/cm². With ADMSCs, viability losses of 40%, 55%, and 40% were observed at 25, 50, and 100 mJ/cm^2 doses at 0 h. At the 24th hour, viability loss was 15% at 100 mJ/cm². At the 48th hour, it is observed that the 100 mJ/cm² dose proliferates rapidly in response to stress. At 50 mJ/cm², viability was 20% less. BMMSCs showed 25% higher viability at 0 h with 25 mJ/cm². At the 24th hour, viability was enhanced by 100%, 150%, and 140% at 25, 50, and 100 mJ/cm². At the 48th hour, cell viability was 50% less than that at 100 mJ/cm². Viability for each hour was compared to the control group.

Gene Expression Analysis

The relative expression levels of genes were analyzed by using qRT-PCR, and *β-actin* as a reference gene (Figure 5). Each treatment group was compared with the control group (C-DMEM). *PPARγ*

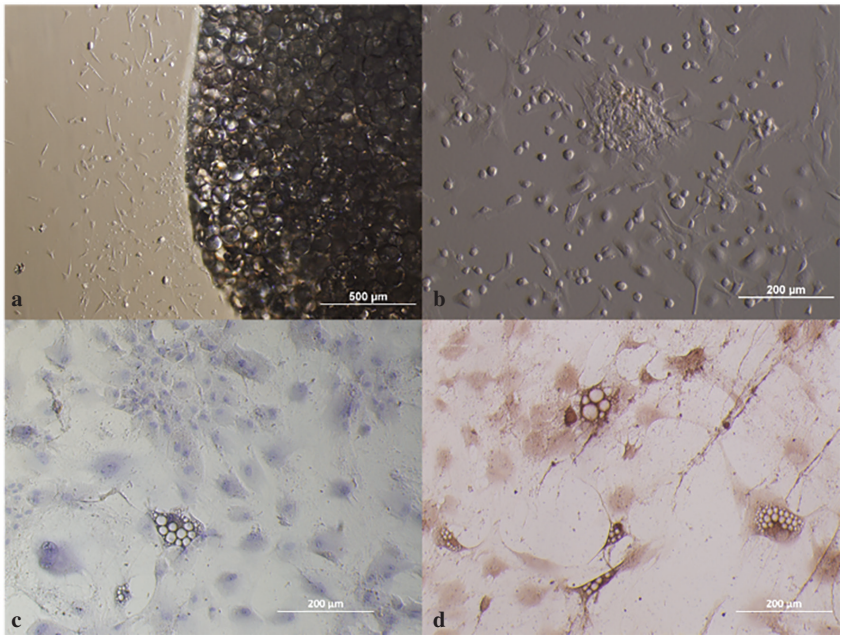

Figure 1. (a) Day 6: Primary isolation of ADMSC; (b) Day 6: Primary isolation of BMMSC; (c) Oil Red O staining of ADMSCs; and (d) BMMSCs were cultured in adipogenic differentiation medium for 28 days.
ADMSC = adipose-derived mesenchymal stem cell; BMMSC = bone marrow mesenchymal stem cell.

expression increased significantly in both adipogenic differentiation control (C-AD DIFF) and UV (UV-AD DIFF) groups (**$p \leq 0.01$ and ***$p \leq 0.001$, respectively) compared to the control group ADMSCs (Figure 5a). A similar trend was seen with BMMSCs for both C-AD DIFF and UV-AD DIFF groups, at $p \leq 0.0001$ (Figure 5b). Additionally, *PPARγ* expression declined in the UV-DMEM group ($p \leq 0.0001$) compared to the control group (Figure 5b). For *Bmal1*, expression level reduced insignificantly in the C-AD DIFF and UV-AD DIFF groups of ADMSCs (Figure 5c), but showed a statistically significant enhancement in BMMSCs of both C-AD DIFF and UV-AD DIFF, at $p \leq 0.05$ and $p \leq 0.01$, respectively (Figure 5d). In addition, *Bmal1* transcription elevated significantly in the ADMSC UV-DMEM group compared to the control ($p \leq 0.05$) (Figure 5c).

Discussion

This study investigated the relationship between adipogenic differentiation and circadian rhythm in UVB-treated MSCs. For this purpose, the cells were first confirmed to be MSCs via characterization and adipogenic differentiation. Then, UVB was applied at three doses to determine the optimum concentration, followed by identifying the day with maximum adipogenic maturity. Then, cell viability, adipogenic differentiation, and the expression of circadian clock-associated genes were analyzed at the molecular level.

Under *in vitro* conditions, the proliferation rate was greater in ADMSCs than in BMMSCs, and ADMSCs more stably maintained stem cell properties, such as self-renewal, proliferation, and differentiation potential after repeated passaging (Christoffers et al., 2024; Zhu et al., 2008). However, BMMSCs demonstrated a markedly higher chondrogenic differentiation capacity (Mohamed-Ahmed et al., 2018), whereas ADMSCs exhibited remarkably greater *in vitro* adipogenic, endothelial differentiation, and angiogenic capacities than BMMSCs in preclinical ischemic injury models (El-Badawy et al., 2016; Yin et al., 2023). Adipose and BMMSCs were chosen for ease of access and adipogenic potential. They are crucial cell sources for regenerative medicine and treating various chronic diseases (Guillamat-Prats, 2021; Lotfy et al., 2023). Differentiation in MSCs starts from the second week, subject to adipogenic differentiation, and completes in the 3rd to 4th week (Mohamed-Ahmed et al., 2018; Ninomiya et al., 2010). In our study, Oil Red O staining performed on day 28 indicated a transformation of MSCs into mature adipocytes.

An appropriate UV dose causes an increase in biomolecules such as growth factors and cytokines in MSCs (Angelina et al., 2025; Yan et al., 2023). Perez et al. (2019) showed that 25 mJ/cm^2 UVB enhanced interleukin -8 release by human MSCs, and that MSCs were more resistant than dermal fibroblasts to UV light. This study identified 25 mJ/cm^2 UVB as the optimum dose at which MSCs could survive. In addition, an earlier study by our group reported the important role of UVA light at 100 mJ/cm^2 in wound healing; it enhances cytokine and growth factor release (Çetin et al., 2023). Another study reported that low-dose UV light did not affect gene expression in human MSCs, but secretory factors and collagen production increased; i.e., the wavelength of UV light and its compatibility with living cells were directly proportional (Wong et al., 2015). Further supporting this correlation, the viability of MSCs treated with 100 mJ/cm^2 UVB declined markedly within the first 24 h, followed by an abnormal increase at the 48th hour. In line with this trend, UV-treated stem cells are effective in wound healing and cell regeneration. UVB light induces a phase shift

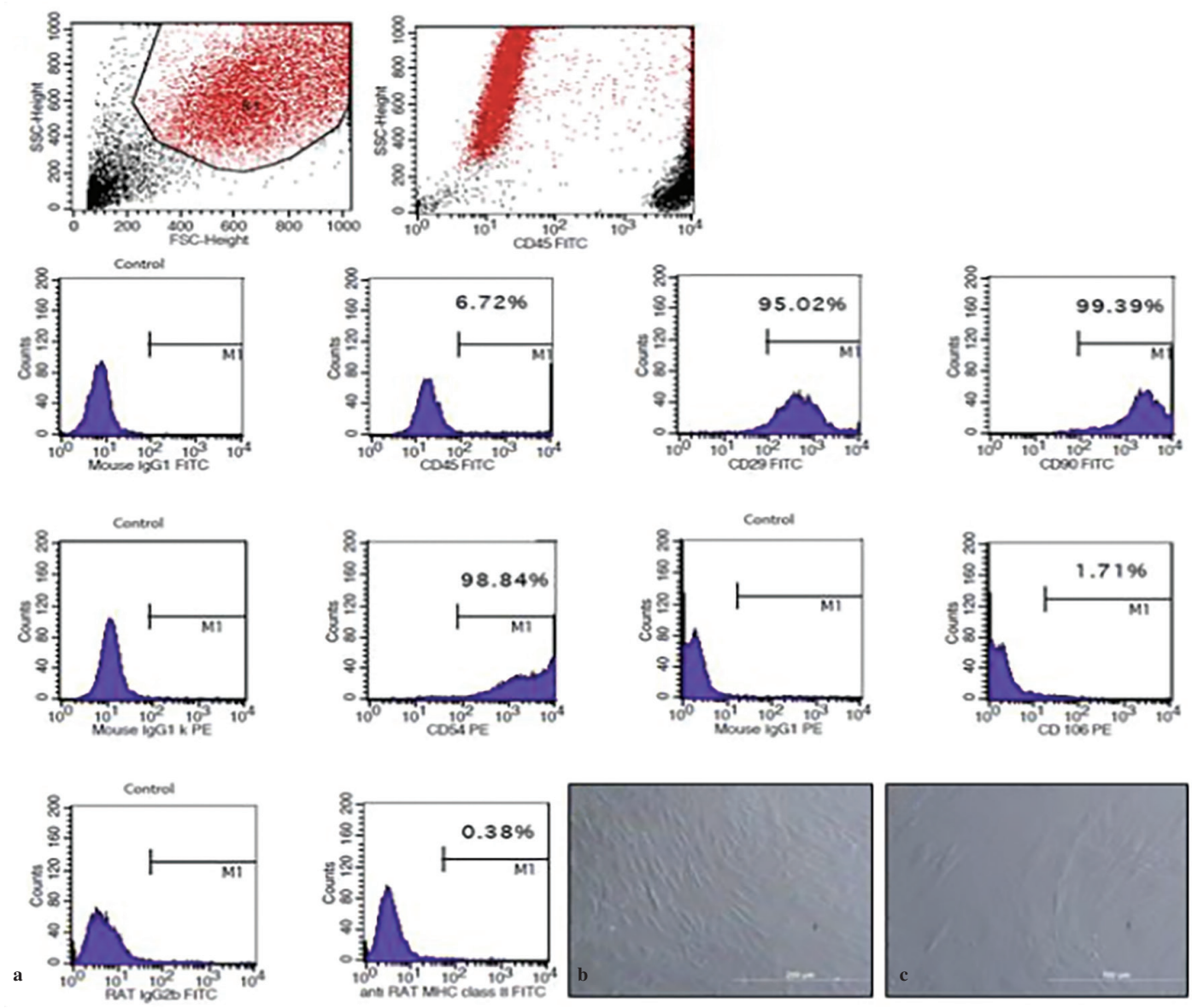

Figure 2. Representative flow cytometry histograms showing expression of MSC surface markers isolated from the P2–P4 population. Most cells (≥95%) were positive for CD54, CD90, and CD29. MSCs were negative for the hematopoietic and immunogenic markers CD45, CD106, and MHC class II, with ≤7% of them expressing these antigens.
CD = cluster of differenti; MHC = major histocompatibility complex; MSC = mesenchymal stem cell.

in the transcription of circadian clock-associated genes such as *Bmal1* and *Per2*, and these changes are associated with sunburn apoptosis, inflammatory responses, and erythema (Lamnis et al., 2024). In this research, UVB was preferred because of its potential to support regenerative processes by enhancing the release of cytokines and growth factors by MSCs. Furthermore, the time point of UV exposure during a 24-hour cycle affects DNA damage and repair through a temporal regulation of the tumor suppressor gene *p53* (Carvalho et al., 2024; Zou et al., 2022). Low levels of DNA repair, especially in the evening when DNA replication is at its peak, render the skin more vulnerable to the harmful effects of UV radiation (Andersen et al., 2023; Su et al., 2024). This process interacts with carcinogenic pathways through receptors directly linked to the circadian rhythm. In contrast, UVB is required for the synthesis of vitamin D3, a compound that affects circadian clock-related genes. Unlike UVB one form of vitamin D3 suppressed *Per2* expression (Lamnis et al., 2024).

Clock gene knock-out reduces cell proliferation and increases apoptosis, whereas *Bmal1* is essential for lineage differentiation (Kaneko et al., 2023; Zhang et al., 2024). Enhanced *Bmal1* expression inhibits adipogenesis, whereas a high *Bmal1* expression pattern was found in mature adipocytes (Lamnis et al., 2024; Xiong et al., 2023). Therefore, the *Bmal1* gene, which plays a central role in stem cell differentiation, was examined in this study. Moreover, *PPARγ* showed circadian expression and was found to be an important peripheral clock activator of the cardiovascular

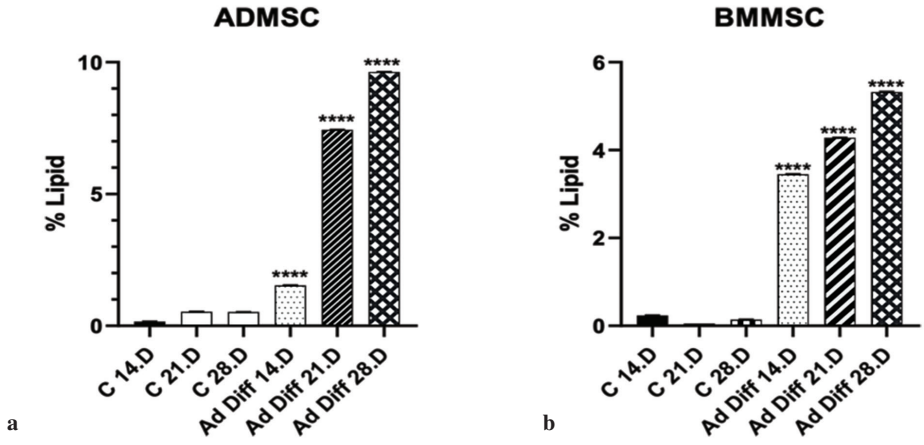

Figure 3. Oil Red O staining indicates the percentage lipid content. It was calculated based on the ratio of the surface area containing oil droplets to the total surface area. (a) % lipid values at days 14, 21, and 28 in ADMSCs and (b) BMMSCs.
AD DIFF = adipogenic differentiation; ADMSCs = adipose-derived mesenchymal stem cells; BMMSCs = bone marrow mesenchymal stem cells; C = control.

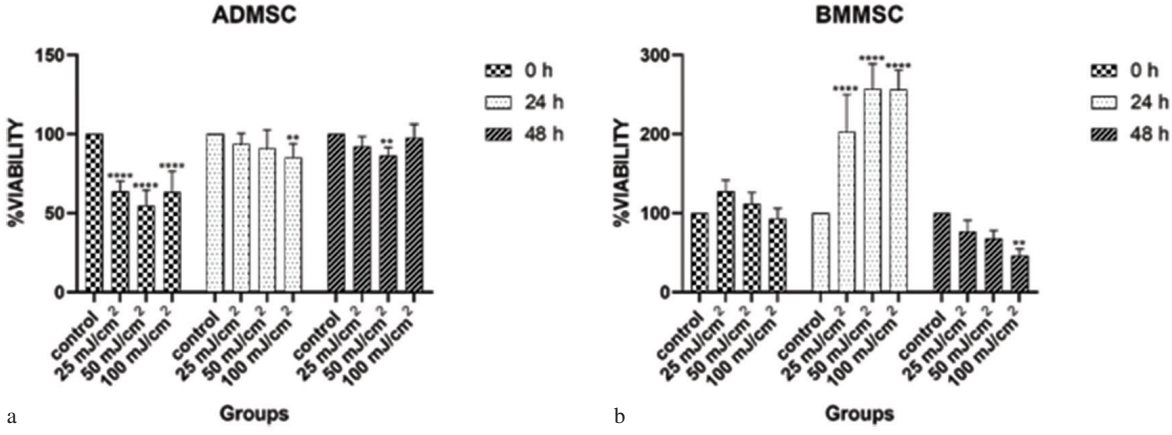

Figure 4. MTT-based cell viability test. Viability at 0, 24, and 48 h in (a) ADMSCs and (b) BMMSCs, graphically presented as MTT results with reference to the control group. UVB was applied at doses of 25, 50, and 100 mJ/cm²; $p \leq 0.05$; $p \leq 0.01$; $p \leq 0.001$; $p \leq 0.0001$.
ADMSCs = adipose-derived mesenchymal stem cells; BMMSCs = bone marrow mesenchymal stem cells; MTT = methyl thiazolyl tetrazolium; UVB = ultraviolet B.

system and metabolism (Ansarin et al., 2023; Li et al., 2025). It has been reported that disruption of *Clock* and *Per2* genes causes a significant decrease in adipogenic differentiation, whereas inhibition of *Clock* or *Per2* leads to an increase in *PPARγ* levels by altering osteocalcin expression (Boucher et al., 2016; Tian et al., 2024). The *Per1* and *Per2* genes have antagonistic effects on *PPARγ* activity, with *Per1* enhancing activity and *Per2* inhibiting recruitment of *PPARγ* to the target promoter (Grimaldi et al., 2010; Zhang et al., 2023). However, the role of *Per2* in adipogenesis depends on a complex regulatory network that interacts with other clock genes, such as *Bmal1* and *REV-ERBα* (Civelek et al., 2023; Gao et al., 2022). Erickson et al. (2024) revealed a relationship between *Per2* expression and the *PPARγ* gene, while Wang et al. (2022) showed that the *PPARγ* gene integrates the obesity and adipocyte clock in a *Bmal1*-dependent manner. In our study, gene expression analysis of *PPARγ* and *Bmal1* statistically showed different expression levels in ADMSCs and BMMSCs. As it is known, circadian clock genes are not found at the same expression level at all times of the day. While *Bmal1* expression increases in the first hours of the day, it is suppressed by the expression of *PER-CRY* genes in the later hours of the day (Li et al., 2023; Mattis et al., 2016). Analyzing MSCs at different times of the day resulted in different *Bmal1* levels. However, our data showed a significant increase between the UV-treated and non-UV-treated groups. The fact that *PPARγ* gene expression was higher in UV-treated groups could mean that UV increased *PPARγ* expression. This could show that UV treatment induced *Bmal1* expression in MSCs.

In vivo, UV exposure may influence circadian rhythm regulation through direct cellular effects and indirect systemic mechanisms involving neuroendocrine signaling, immune responses, and central clock synchronization. Therefore, whole-animal models

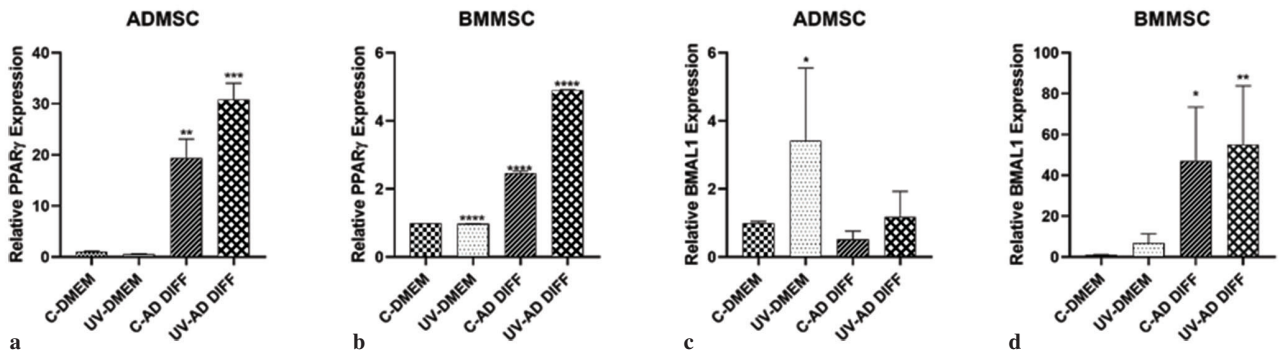

Figure 5. Expression levels of *PPARγ* and *Bmal1*. (a) *PPARγ* expression in ADMSCs; (b) in BMMSCs; (c) *Bmal1* expression in ADMSCs; and (d) in BMMSCs ($p \leq 0.05$; $p \leq 0.01$; $p \leq 0.001$; $p \leq 0.0001$).
AD DIFF = adipogenic differentiation; ADMSCs = adipose-derived mesenchymal stem cells; BMMSCs = bone marrow mesenchymal stem cells; C = control.

could provide valuable insight into tissue-specific and systemic circadian responses to UV exposure. Although the overall direction of UV-induced modulation of circadian clock genes is expected to be consistent with *in vitro* findings, the magnitude and temporal dynamics of these effects may differ *in vivo* due to hormonal regulation, metabolic status, and inter-organ communication. In this context, the *in vitro* MSCs model used in the present study allows precise control of UV dose and exposure timing, enabling the investigation of direct molecular mechanisms underlying UVB-induced regulation of adipogenic differentiation and circadian clock genes. The present findings, therefore, establish a mechanistic foundation that may inform future *in vivo* studies aimed at evaluating the physiological relevance of UV-induced circadian modulation.

Originality of this study lies in its simultaneous evaluation of *Bmal1* and *PPARγ* expression in MSCs obtained from different tissue sources under UV exposure. While previous studies have demonstrated the independent roles of clock genes in determining stem cell fate and adipogenic differentiation, research integrating environmental cues, such as UV irradiation, with circadian-adipogenic gene interactions is limited. In particular, the literature has not sufficiently explored comparative analyses of ADMSCs and BMMSCs in terms of circadian gene sensitivity and adipogenic potential. This study offers a new perspective by demonstrating that UV exposure is associated with coordinated changes in *Bmal1* and *PPARγ* expression patterns in MSC types. These findings suggest a potential regulatory role of light-related environmental stimuli in the circadian mechanism and lineage determination processes of stem cells. Additionally, observing tissue-specific expression differences between ADMSCs and BMMSCs helps us understand the intrinsic heterogeneity in the circadian regulation and adipogenic potential of MSCs. Collectively, these findings expand current knowledge on circadian–metabolic gene interactions in stem cells and suggest that UV-mediated circadian modulation represents a potential regulatory layer influencing the dynamics of adipogenic differentiation.

This study has several strengths that enhance the reliability and interpretability of its findings. First, the simultaneous investigation of circadian clock regulation and adipogenic differentiation provides a comprehensive perspective on stem cell biology, allowing the evaluation of metabolic-temporal interactions within a unified experimental framework. Second, the inclusion of MSCs (ADMSCs and BMMSCs) derived from different tissue sources allows the comparative assessment of tissue-specific variability, contributing to the understanding of intrinsic heterogeneity of the MSCs. Third, the inclusion of UV exposure as an environmental stimulus provides a physiologically relevant modulatory factor, facilitating the investigation of how external cues interact with circadian and differentiation-related molecular pathways. However, several limitations should be considered when interpreting the results. The study was conducted under *in vitro* conditions, which may not fully reflect the complex systemic and microenvironmental effects present *in vivo*. The assessment of circadian genes at specific time points rather than longitudinal rhythmic profiling limits the findings regarding oscillation dynamics. Future studies incorporating time series analysis, functional clock measurements, and *in vivo* validation models will help further elucidate the biological significance of the observed findings.

Conclusion

Within the scope of this study, adipogenic differentiation and expression of circadian rhythm-associated genes were investigated at UVB doses optimal for maintaining the viability of MSCs of two different origins. Studies indicate the relationships between circadian rhythm and UV light, or adipogenic differentiation and circadian rhythm. However, none have addressed the latter in UVB-treated MSCs. In summary, this study demonstrated that the optimum UVB dose induces adipogenesis in MSCs and regulates the circadian rhythm.

The role of *Bmal1* in stabilizing *PPARγ* transcriptional activity and the feedback effect of *PPARγ* on the circadian rhythm are fundamental mechanisms determining the cell's differentiation fate. In this context, the patterns observed reinforce the concept of a coordinated circadian–metabolic regulatory axis in which adipogenic programming and clock gene activity, including *Bmal1*, are dynamically integrated.

These findings provide a mechanistic basis for future studies aiming to evaluate how similar responses would unfold under physiological conditions (*in vivo*) by elucidating how the *Bmal1–PPARγ* interaction is reprogrammed by UVB.

These findings provide a mechanistic basis for future *in vivo* studies aimed at evaluating whether similar UV-induced circadian and differentiation responses occur under physiological conditions.

Acknowledgement

The authors would like to thank the Akbay Lab for their valuable support and contributions to this study. The authors also gratefully acknowledge The Scientific and Technological Research Council of Türkiye (TÜBİTAK) for its financial support.

Ethics

Ethics Committee Approval: The animals used were obtained post-approval from the Hacettepe University Animal Ethics Committee (number 2021/05-05; dated June 22, 2021).

Data Sharing Statement: All data are available within the study.

Footnotes

Authorship Contributions: Conceptualization: A.K. and E.A.Ç.; Design/methodology: A.K. and E.A.Ç.; Execution/investigation: A.K., E.T., B.E., and E.A.Ç.; Resources/materials: A.K. and E.A.Ç.; Data acquisition: A.K., E.T., B.E., and E.A.Ç.; Data analysis/interpretation: A.K., E.T., B.E., and E.A.Ç.; Writing – original draft: A.K., E.T., B.E., and E.A.Ç.; Writing – review & editing/critical revision: A.K., E.T., B.E., and E.A.Ç.

Conflict of Interest: The author(s) have no conflicts of interest to declare.

Funding: This research was supported by the 2209-A University Students Research Projects Support Programme of TÜBİTAK (project no: 1919B012216469). The project was conducted by Afra Keban under the supervision of the corresponding author, Esin Akbay Çetin.

References

Andersen, B., Duan, J., & Karri, S. S. (2023). How and why the circadian clock regulates proliferation of adult epithelial stem cells. *Stem Cells, 41*(4), 319–327. https://doi.org/10.1093/stmcls/sxad013

Angelina, J., Putra, A., Trisnadi, S., Hermansyah, D., Setiawan, E., Sumarawati, T., & Amalina, N. D. (2025). Hypoxia-conditioned mesenchymal stem cells (MSC) exosomes attenuate ultraviolet-B (UVB)-mediated malondialdehyde (MDA) and matrix metalloproteinase-1 (MMP-1) upregulation in collagen loss models. *Medicinski Glasnik, 22*(1). https://doi.org/10.17392/1923-22-01

Ansarin, A., Mahdavi, A. M., Javadivala, Z., Shanehbandi, D., Zarredar, H., & Ansarin, K. (2023). The cross-talk between leptin and circadian rhythm signaling proteins in physiological processes: A systematic review. *Molecular Biology Reports, 50*(12), 10427–10443. https://doi.org/10.1007/s11033-023-08887-3

Boucher, H., Vanneaux, V., Domet, T., Parouchev, A., & Larghero, J. (2016). Circadian clock genes modulate human bone marrow mesenchymal stem cell differentiation, migration and cell cycle. *PLOS ONE, 11*(1), e0146674. https://doi.org/10.1371/journal.pone.0146674

Carvalho, C., Silva, R., Melo, T. M. V. D. P. e, Inga, A., & Saraiva, L. (2024). P53 and the ultraviolet radiation-induced skin response: Finding the light in the darkness of triggered carcinogenesis. *Cancers, 16*(23), 3978. https://doi.org/10.3390/cancers16233978

Česnik, A. B., & Švajger, U. (2024). The issue of heterogeneity of MSC-based advanced therapy medicinal products-a review. *Frontiers in Cell and Developmental Biology, 12*, 1400347. https://doi.org/10.3389/fcell.2024.1400347

Christoffers, S., Seiler, L., Wiebe, E., & Blume, C. (2024). Possibilities and efficiency of MSC co-transfection for gene therapy. *Stem Cell Research & Therapy, 15*(1), 150. https://doi.org/10.1186/s13287-024-03757-6

Civelek, E., Ozturk Civelek, D., Akyel, Y. K., Kaleli Durman, D., & Okyar, A. (2023). Circadian dysfunction in adipose tissue: Chronotherapy in metabolic diseases. *Biology, 12*(8), 1077. https://doi.org/10.3390/biology12081077

Çetin, E. A., Babayiğit, E. H., Özdemir, A. Y., Erfen, Ş., & Onur, M. A. (2023). Investigation of UV-treated mesenchymal stem cells in an *in vitro* wound model. *In Vitro Cellular & Developmental Biology-Animal, 59*(5), 331–345. https://doi.org/10.1007/s11626-023-00772-4

El-Badawy, A., Amer, M., Abdelbaset, R., Sherif, S. N., Abo-Elela, M., Ghallab, Y. H., Abdelhamid, H., Ismail, Y., & El-Badri, N. (2016). Adipose stem cells display higher regenerative capacities and more adaptable electro-kinetic properties compared to bone marrow-derived mesenchymal stromal cells. *Scientific Reports, 6*, 37801. https://doi.org/10.1038/srep37801

Erickson, M. L., Dobias, D., Keleher, M. R., Dabelea, D., Bergman, B. C., Broussard, J. L., & Boyle, K. E. (2024). *In vitro* circadian clock gene expression assessments in mesenchymal stem cells from human infants: A pilot study. *Nutrients, 16*(1), 52. https://doi.org/10.3390/nu16010052

Ezati, P., Khan, A., Priyadarshi, R., Bhattacharya, T., Tammina, S. K., & Rhim, J.-W. (2023). Biopolymer-based UV protection functional films for food packaging. *Food Hydrocolloids, 142*, 108771. https://doi.org/10.1016/j.foodhyd.2023.108771

Gao, W., Li, R., Ye, M., Zhang, L., Zheng, J., Yang, Y., Wei, X., & Zhao, Q. (2022). The circadian clock has roles in mesenchymal stem cell fate decision. *Stem Cell Research & Therapy, 13*(1), 200. https://doi.org/10.1186/s13287-022-02878-0

Goodenow, D., Greer, A. J., Cone, S. J., & Gaddameedhi, S. (2022). Circadian effects on UV-induced damage and mutations. *Mutation Research - Reviews in Mutation Research, 789*, 108413. https://doi.org/10.1016/j.mrrev.2022.108413

Göncü, B., & Öztürk, D. (2019). HT29 hücre hattında sirkadiyen ritme bağlı gen ifadesinin kontrolünde referans gen farklılığının senkronizasyondaki rolü. *Erzincan Üniversitesi Fen Bilimleri Enstitüsü Dergisi, 12*(3), 1370–1380. https://doi.org/10.18185/erzifbed.523088

Grimaldi, B., Bellet, M. M., Katada, S., Astarita, G., Hirayama, J., Amin, R. H., Granneman, J. G., Piomelli, D., Leff, T., & Sassone-Corsi, P. (2010). PER2 controls lipid metabolism by direct regulation of *PPARγ*. *Cell Metabolism, 12*(5), 509–520. https://doi.org/10.1016/j.cmet.2010.10.005

Guillamat-Prats, R. (2021). The role of MSC in wound healing, scarring, and regeneration. *Cells, 10*(7), 1729.

Kaneko, H., Kaitsuka, T., & Tomizawa, K. (2023). Artificial induction of circadian rhythm by combining exogenous BMAL1 expression and polycomb repressive complex 2 inhibition in human induced pluripotent stem cells. *Cellular and Molecular Life Sciences, 80*(8), 200. https://doi.org/10.1007/s00018-023-04847-z

Lamnis, L., Christofi, C., Stark, A., Palm, H., Roemer, K., Vogt, T., & Reichrath, J. (2024). Differential regulation of circadian clock genes by UV-B radiation and 1,25-dihydroxyvitamin D: A pilot study during different stages of skin photocarcinogenesis. *Nutrients, 16*(2), 254. https://doi.org/10.3390/nu16020254

Li, W., Wang, Y., Liu, C., Yu, Y., Xu, L., & Dong, B. (2025). Evaluation of the regulatory effect of the pan-PPAR agonist chiglitazar on the dawn phenomenon. *Diabetes Therapy, 16*(4), 731–748. https://doi.org/10.1007/s13300-025-01708-9

Li, Z., Li, Y., Xu, X., Gu, J., Chen, H., & Gui, Y. (2023a). Exosomes rich in Wnt5 improved circadian rhythm dysfunction via enhanced PPARγ activity in the 6-hydroxydopamine model of Parkinson's disease. *Neuroscience Letters, 802*, 137139. https://doi.org/10.1016/j.neulet.2023.137139

Li, Z., Yan, T., & Fang, X. (2023b). Low-dimensional wide-bandgap semiconductors for UV photodetectors. *Nature Reviews Materials, 8*, 587–603. https://doi.org/10.1038/s41578-023-00583-9

Liao, W., Duan, X., Xie, F., Zheng, D., Yang, P., Wang, X., & Hu, Z. (2023). 3D-bioprinted double-crosslinked angiogenic alginate/chondroitin sulfate patch for diabetic wound healing. *International Journal of Biological Macromolecules, 236*, 123952. https://doi.org/10.1016/j.ijbiomac.2023.123952

Lotfy, A., AboQuella, N. M., & Wang, H. (2023). Mesenchymal stromal/stem cell (MSC)-derived exosomes in clinical trials. *Stem Cell Research & Therapy, 14*(1), 66. https://doi.org/10.1186/s13287-023-03287-7

Lotfy, A., El-Sherbiny, Y. M., Cuthbert, R., Jones, E., & Badawy, A. M. (2019). Comparative study of biological characteristics of mesenchymal stem cells isolated from mouse bone marrow and peripheral blood. *Biomedical Reports, 11*, 165–170. https://doi.org/10.3892/br.2019.1236

Mattis, J., & Sehgal, A. (2016). Circadian rhythms, sleep, and disorders of aging. *Trends in Endocrinology & Metabolism, 27*(4), 192–203. https://doi.org/10.1016/j.tem.2016.02.003

Mens, M. M. J., & Ghanbari, M. (2018). Cell cycle regulation of stem cells by microRNAs. *Stem Cell Reviews and Reports, 14*, 309–322. https://doi.org/10.1007/s12015-018-9808-y

Mohamed-Ahmed, S., Fristad, I., Lie, S. A., Suliman, S., Mustafa, K., Vindenes, H., & Idris, S. B. (2018). Adipose-derived and bone marrow mesenchymal stem cells: A donor-matched comparison. *Stem Cell Research & Therapy, 9*(1), 168. https://doi.org/10.1186/s13287-018-0914-1

Montaigne, D., Butruille, L., & Staels, B. (2021). PPAR control of metabolism and cardiovascular functions. *Nature Reviews Cardiology, 18*(12), 809–823. https://doi.org/10.1038/s41569-021-00569-6

Ninomiya, Y., Sugahara-Yamashita, Y., Nakachi, Y., Tokuzawa, Y., Okazaki, Y., & Nishiyama, M. (2010). Development of a rapid culture method to induce adipocyte differentiation of human bone marrow-derived mesenchymal stem cells. *Biochemical and Biophysical Research Communications, 394*(2), 303–308. https://doi.org/10.1016/j.bbrc.2010.03.001

Niyaz, M., Gürpınar, Ö. A., Günaydın, S., & Onur, M. A. (2012). Isolation, culturing and characterization of rat adipose tissue-derived mesenchymal stem cells: A simple technique. *Turkish Journal of Biology, 36*(6), 658–664. https://doi.org/10.3906/biy-1109-31

Perez, R. L., Brauer, J., Rühle, A., Trinh, T., Sisombath, S., Wuchter, P., Grosu, A. L., Debus, J., Saffrich, R., Huber, P. E., & Nicolay, N. H. (2019). Human mesenchymal stem cells are resistant to UV-B irradiation. *Scientific Reports, 9*(1), 20000. https://doi.org/10.1038/s41598-019-56591-9

Pittenger, M. F., Discher, D. E., Péault, B. M., Phinney, D. G., Hare, J. M., & Caplan, A. I. (2019). Mesenchymal stem cell perspective: Cell biology to clinical progress. *NPJ Regenerative Medicine, 4*, 22. https://doi.org/10.1038/s41536-019-0083-6

Putthanbut, N., Su, P. A. B., Lee, J. Y., & Borlongan, C. V. (2025). Circadian rhythms in stem cells and their therapeutic potential. *Stem Cell Research & Therapy, 16*(1), 85. https://doi.org/10.1186/s13287-025-04178-9

Ra, K., Park, S. C., & Lee, B. C. (2023). Female reproductive aging and oxidative stress: Mesenchymal stem cell conditioned medium as a promising antioxidant. *International Journal of Molecular Sciences, 24*(5), 5053. https://doi.org/10.3390/ijms24055053

Sani, M. A., Khezerlou, A., Tavassoli, M., Abedini, A. H., & McClements, D. J. (2024). Development of sustainable UV-screening food packaging materials: A review of recent advances. *Trends in Food Science & Technology, 145*, 104366. https://doi.org/10.1016/j.tifs.2024.104366

Sevim, H., Kocaefe, Y. Ç., Onur, M. A., Uçkan-Çetinkaya, D., & Gürpınar, Ö. A. (2018). Bone marrow derived mesenchymal stem cells ameliorate inflammatory response in an *in vitro* model of familial hemophagocytic lymphohistiocytosis 2. *Stem Cell Research & Therapy, 9*(1), 198. https://doi.org/10.1186/s13287-018-0941-y

Su, Z., Hu, Q., Li, X., Wang, Z., & Xie, Y. (2024). The influence of circadian rhythms on DNA damage repair in skin photoaging. *International Journal of Molecular Sciences, 25*(20), 10926. https://doi.org/10.3390/ijms252010926

Takahashi, J. S. (2017). Transcriptional architecture of the mammalian circadian clock. *Nature Reviews Genetics, 18*(3), 164–179. https://doi.org/10.1038/nrg.2016.150

Tian, Y., Luan, X., & Yang, K. (2024). Chronotherapy involving rosiglitazone regulates the phenotypic switch of vascular smooth muscle cells by shifting the phase of TNF-α rhythm through triglyceride accumulation in macrophages. *Heliyon, 10*(10), e30708. https://doi.org/10.1016/j.heliyon.2024.e30708

Vilar, A., Hodgson-Garms, M., & Frith, J. E. (2023). Substrate mechanical properties bias MSC paracrine activity and therapeutic potential. *Acta Biomaterialia, 168*, 1–15. https://doi.org/10.1016/j.actbio.2023.06.041

Wang, S., Lin, Y., Gao, L., Yang, Z., Lin, J., Ren, S., Li, F., Chen, J., Wang, Z., Dong, Z., Sun, P., & Wu, B. (2022). PPAR-γ integrates obesity and adipocyte clock through epigenetic regulation of Bmal1. *Theranostics, 12*(4), 1589–1606. https://doi.org/10.7150/thno.69054

Wong, D. Y., Ranganath, T., & Kasko, A. M. (2015). Low-dose, long-wave UV light does not affect gene expression of human mesenchymal stem cells. *PLOS ONE, 10*(9), e0139307. https://doi.org/10.1371/journal.pone.0139307

Xiong, X., Kiperman, T., Li, W., Dhawan, S., Lee, J., Yechoor, V., & Ma, K. (2023). The clock-modulatory activity of nobiletin suppresses adipogenesis via Wnt signaling. *Endocrinology, 164*(8), bqad096. https://doi.org/10.1210/endocr/bqad096

Yan, T., Huang, L., Yan, Y., Zhong, Y., Xie, H., & Wang, X. (2023). MAPK/AP-1 signaling pathway is involved in the protection mechanism of bone marrow mesenchymal stem cells-derived exosomes against ultraviolet-induced photoaging in human dermal fibroblasts. *Skin Pharmacology and Physiology, 36*(2), 98–106. https://doi.org/10.1159/000529551

Yin, X., Lin, L., Fang, F., Zhang, B., & Shen, C. (2023). Mechanisms and optimization strategies of paracrine exosomes from mesenchymal stem cells in ischemic heart disease. *Stem Cells International, 2023*, 6500831. https://doi.org/10.1155/2023/6500831

Zeng, Y., Guo, Z., Wu, M., Chen, F., & Chen, L. (2024). Circadian rhythm regulates the function of immune cells and participates in the development of tumors. *Cell Death Discovery, 10*(1), 199. https://doi.org/10.1038/s41420-024-01960-1

Zhang, L., Zhang, C., Zheng, J., Wang, Y., Wei, X., Yang, Y., & Zhao, Q. (2024). miR-155-5p/Bmal1 modulates the senescence and osteogenic differentiation of mouse BMSCs through the Hippo signaling pathway. *Stem Cell Reviews and Reports, 20*(2), 554–567. https://doi.org/10.1007/s12015-023-10666-3

Zhang, Y., Li, Y., Gao, N., Gong, Y., Shi, W., & Wang, X. (2023). Transcriptome and metabolome analyses reveal perfluorooctanoic acid-induced kidney injury by interfering with PPAR signaling pathway. *International Journal of Molecular Sciences, 24*(14), 11503. https://doi.org/10.3390/ijms241411503

Zhu, Y., Liu, T., Song, K., Fan, X., Ma, X., & Cui, Z. (2008). Adipose-derived stem cell: A better stem cell than BMSC. *Cell Biochemistry and Function, 26*(6), 664–675. https://doi.org/10.1002/cbf.1488

Zhu, Z., Guo, L., Yeltai, N., Xu, H., & Zhang, Y. (2022). Chemokine (C-C motif) ligand 2-enhanced adipogenesis and angiogenesis of human adipose-derived

stem cell and human umbilical vein endothelial cell co-culture system in adipose tissue engineering. *Journal of Tissue Engineering and Regenerative Medicine, 16*(2), 163–176. https://doi.org/10.1002/term.3264

Zou, X., Zou, D., Li, L., Yu, R., Li, X., Du, X., Guo, J., Wang, K., & Liu, W. (2022). Multi-omics analysis of an in vitro photoaging model and protective effect of umbilical cord mesenchymal stem cell-conditioned medium. Stem Cell Research & Therapy, 13, 435. https://doi.org/10.1186/s13287-022-03137-y